

Spatially Coupled Turbo Codes

Saeedeh Moloudi[†], Michael Lentmaier[‡], and Alexandre Graell i Amat[‡]

[†]Department of Electrical and Information Technology, Lund University, Lund, Sweden

[‡]Department of Signals and Systems, Chalmers University of Technology, Gothenburg, Sweden
{saeedeh.moloudi,michael.lentmaier}@eit.lth.se, alexandre.graell@chalmers.se

Abstract—In this paper, we introduce the concept of spatially coupled turbo codes (SC-TCs), as the turbo codes counterpart of spatially coupled low-density parity-check codes. We describe spatial coupling for both Berrou *et al.* and Benedetto *et al.* parallel and serially concatenated codes. For the binary erasure channel, we derive the exact density evolution (DE) equations of SC-TCs by using the method proposed by Kurkoski *et al.* to compute the decoding erasure probability of convolutional encoders. Using DE, we then analyze the asymptotic behavior of SC-TCs. We observe that the belief propagation (BP) threshold of SC-TCs improves with respect to that of the uncoupled ensemble and approaches its maximum a posteriori threshold. This phenomenon is especially significant for serially concatenated codes, whose uncoupled ensemble suffers from a poor BP threshold.

I. INTRODUCTION

Low-density parity-check (LDPC) convolutional codes [1], also known as spatially coupled LDPC (SC-LDPC) codes [2], can be obtained from a sequence of individual LDPC block codes by distributing the edges of their Tanner graphs over several adjacent blocks [3]. The resulting spatially coupled codes exhibit a threshold saturation phenomenon, which has attracted a lot of interest in the past few years: the threshold of an iterative belief propagation (BP) decoder, obtained by density evolution (DE), is improved to that of the optimal maximum-a-posteriori (MAP) decoder [2], [3]. As a consequence, it is possible to achieve capacity with simple regular LDPC codes, which show without spatial coupling a significant gap between BP and MAP threshold.

The concept of spatial coupling is not limited to LDPC codes. Spatially coupled turbo-like codes, for example, can be obtained by replacing the block-wise permutation of a turbo code by a convolutional permutation [4]. In combination with a windowed decoder for the component code, a continuous streaming implementation is possible [5]. The self-concatenated convolutional codes in [6] are closely related structures as well. A variant of spatially coupled self-concatenated codes with block-wise processing, called laminated codes was considered in [7]. They have the advantage that an implementation similar to uncoupled turbo codes is possible, without the need for a streaming implementation of the decoder. A block-wise version of braided convolutional codes [8], a class of spatially coupled codes with convolutional components, has recently been analyzed in [9].

The aim of this paper is to investigate the impact of spatial coupling on the thresholds of *classical* turbo codes. For this

purpose we introduce some special block-wise spatially coupled ensembles of parallel concatenated codes (SC-PCCs) and serially concatenated codes (SC-SCCs), which are spatially coupled versions of the ensembles by Berrou *et al.* [10] and Benedetto *et al.* [11], respectively. With a slight abuse of the term, we call both parallel and serial ensembles spatially coupled turbo codes (SC-TCs). For these ensembles we derive exact DE equations from the transfer functions of the component decoders [12], [13] and perform a threshold analysis for the binary erasure channel (BEC), analogously to [3], [9]. To compare the results for SC-PCC and SC-SCC ensembles with each other some ensembles with puncturing are also considered. The BP thresholds of the different ensembles are presented and compared to the MAP thresholds for different coupling memories.

II. SPATIALLY COUPLED TURBO CODES

In this section, we introduce spatially coupled turbo codes. We first describe spatial coupling for both parallel and serially concatenated codes, and then address their iterative decoding.

A. Spatially Coupled Parallel Concatenated Codes

We consider the spatial coupling of $R = 1/3$ parallel concatenated codes, built from the parallel concatenation of two rate-1/2 recursive systematic convolutional encoders, denoted by C_U and C_L (see Fig. 1). For simplicity, we describe spatial coupling with coupling memory $m = 1$. Consider a collection of L turbo encoders at time instants $t = 1, \dots, L$, as illustrated in Fig. 1(a). L is called the coupling length. We denote by \mathbf{u}_t the information sequence, and by \mathbf{v}_t^U and \mathbf{v}_t^L the code sequences of C_U and C_L , respectively, at time t . The output of the turbo encoder is given by the tuple $\mathbf{v}_t = (\mathbf{u}_t, \mathbf{v}_t^U, \mathbf{v}_t^L)$. A SC-PCC ensemble (with $m = 1$) is obtained by connecting each turbo code in the chain to the one on the left and to the one on the right as follows. Divide the information sequence \mathbf{u}_t into two sequences, $\mathbf{u}_{t,A}$ and $\mathbf{u}_{t,B}$ by a demultiplexer. Also divide a copy of the information sequence, which is properly reordered by the permutation Π_t , into two sequences, $\mathbf{u}_{t,A'}$ and $\mathbf{u}_{t,B'}$ by another demultiplexer. At time t , the information sequence at the input of encoder C_U is $(\mathbf{u}_{t,A}, \mathbf{u}_{t-1,B})$, properly reordered by a permutation Π_t^U . Likewise, the information sequence at the input of encoder C_L is $(\mathbf{u}_{t,A'}, \mathbf{u}_{t-1,B'})$, properly reordered by the permutation Π_t^L . In Fig. 1 the blue lines represent the information bits from the current time slot t that are used in the next time slot $t+1$ and the green lines represent the information bits from the

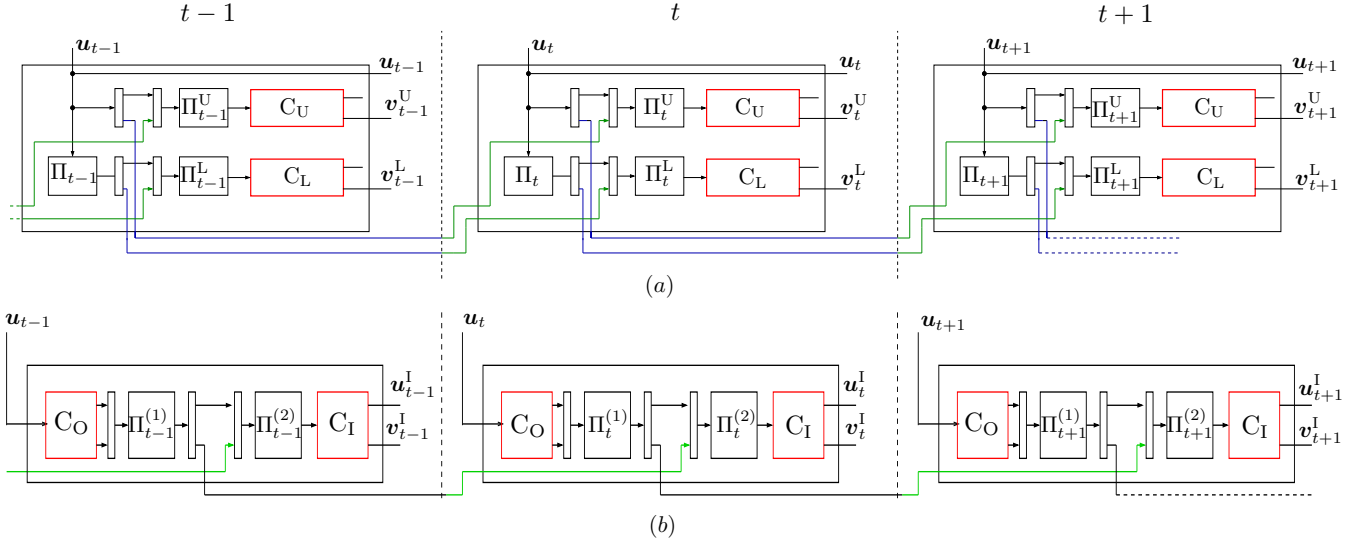


Fig. 1. Block diagram of the encoder of a spatially coupled turbo code for coupling memory $m = 1$. (a) parallel concatenation (b) serial concatenation.

previous time slot $t - 1$. In order to terminate the encoder of the SC-PCC to the zero state, the information sequences at the end of the chain are chosen in such a way that the output sequence at time $t = L + 1$ becomes $v_{L+1} = \mathbf{0}$. Analogously to conventional convolutional codes this results in a rate loss that becomes smaller as L increases.

Using the procedure described above a coupled chain (a convolutional structure over time) of L turbo encoders with coupling memory $m = 1$ is obtained. An extension to larger coupling memories $m > 1$ is presented in Section IV.

B. Spatially Coupled Serially Concatenated Codes

We consider the coupling of serially concatenated codes (SCCs) built from the serial concatenation of two rate-1/2 recursive systematic convolutional encoders. The overall code rate of the uncoupled ensemble is therefore $R = 1/4$. A block diagram of the encoder is depicted in Fig. 1(b) for coupling memory $m = 1$. As for SC-PCCs, let u_t be the information sequence at time t . Also, denote by $v_t^O = (v_t^{O,s}, v_t^{O,p}) = (u_t, v_t^{O,p})$ and v_t^I the encoded sequence at the output of the outer and inner encoder, respectively, and by \tilde{v}_t^O the sequence v_t^O after permutation. The SC-SCC with $m = 1$ is constructed as follows. Consider a collection of L SCCs at time instants $t = 1, \dots, L$. Divide the sequence \tilde{v}_t^O into two parts, $\tilde{v}_{t,A}^O$ and $\tilde{v}_{t,B}^O$. Then, at time t the sequence at the input of the inner encoder C_I is $(\tilde{v}_{t,A}^O, \tilde{v}_{t-1,B}^O)$. In order to terminate the encoder of the SC-SCC to the zero state, the information sequences at the end of the chain are chosen in such a way that the output sequence at time $t = L + 1$ becomes $v_{L+1}^I = \mathbf{0}$.

Using this construction method, a coupled chain of L SCCs with coupling memory $m = 1$ is obtained. An extension to larger coupling memories $m > 1$ is presented in Section IV.

C. Iterative decoding

As standard turbo codes, SC-TCs can be decoded using iterative message passing (belief propagation) decoding, where

the component encoders of each turbo code are decoded using the BCJR algorithm. The BP decoding of SC-PCCs can be easily visualized with the help of Fig. 2, which shows the factor graph of a single section of the SC-PCC. We denote by D_U and D_L the decoder of the upper and lower encoder, respectively.

The decoder D_U receives at its input information from the channel for both systematic and parity bits. Furthermore, it also receives a-priori information on the systematic bits from other decoders. As described above, at time t the information sequence at the input of C_U consists of two parts, $u_{t,A}$ and $u_{t-1,B}$. Correspondingly, D_U at time instant t receives a priori information from D_L at time instants $t - 1$, t and $t + 1$. Based on the information from the channel and from the companion decoders, D_U computes the extrinsic information on the systematic bits using the BCJR algorithm. Since the structure of SC-PCCs is symmetric, the decoding of the lower encoder is performed in an identical manner.

Similarly to SC-PCCs, the decoding SC-SCCs can also be described with the help of a factor graph. The factor graph of a section of a SC-SCC with $m = 1$ is shown in Fig. 3.

III. DENSITY EVOLUTION ANALYSIS ON THE BEC

In this section, we analyze the asymptotic performance of SC-TCs using DE. We consider transmission over a BEC with erasure probability ϵ , denoted by $\text{BEC}(\epsilon)$. We derive the exact DE equations for both (unpunctured) SC-PCCs and SC-SCCs and discuss the modification of the equations when puncturing is applied for achieving higher rates.

A. Spatially Coupled Parallel Concatenated Codes

Let $p_{U,s}$ and $p_{L,s}$ be the average (extrinsic) erasure probability on the systematic bits at the output of the upper and lower decoder, respectively. Likewise, we define $p_{U,p}$ and $p_{L,p}$ for the parity bits.

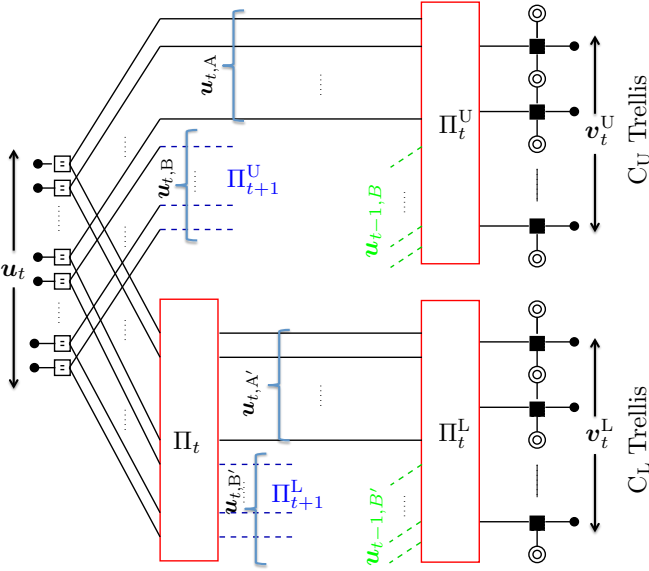


Fig. 2. Factor graph of a single section of a SC-PCC.

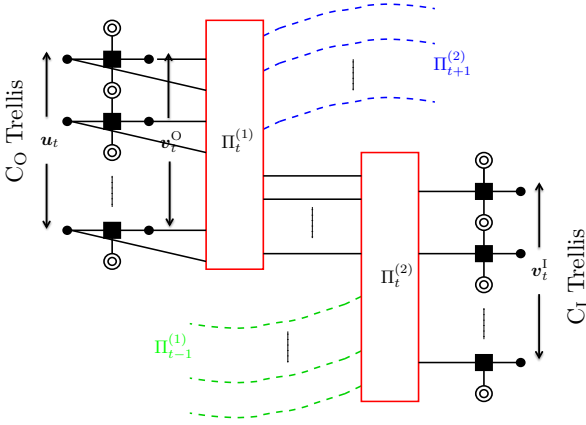


Fig. 3. Factor graph of a single section of a SC-SCC

The erasure probabilities $p_{U,s}$ and $p_{U,p}$ at iteration i and time instant t can be written as

$$p_{U,s}^{(i,t)} = f_{U,s}(q_L^{(i-1)}, \epsilon) \quad (1)$$

$$p_{U,p}^{(i,t)} = f_{U,p}(q_L^{(i-1)}, \epsilon), \quad (2)$$

where

$$q_L^{(i-1)} = \epsilon \cdot \frac{2p_{L,s}^{(i-1,t)} + p_{L,s}^{(i-1,t-1)} + p_{L,s}^{(i-1,t+1)}}{4}, \quad (3)$$

and $f_{U,s}$ and $f_{U,p}$ denote the upper decoder transfer functions for the systematic and parity bits, respectively.

Note that the upper decoder transfer function at time t depends on both the channel erasure probability and the extrinsic erasure probability on the systematic bits from the lower decoder at time instants t , $t-1$ and $t+1$, due to the coupling. Because of the symmetric design, the lower decoder update is identical to that of the upper decoder by interchanging p_U and p_L , and substituting $q_L \leftarrow q_U$ in (1)–(3).

Finally, the a-posteriori erasure probability on the information bits at time t and iteration i is¹

$$p_a^{(i,t)} = \epsilon \cdot \frac{p_{U,s}^{(i,t)} p_{L,s}^{(i,t)} + p_{U,s}^{(i,t)} p_{L,s}^{(i,t+1)} + p_{U,s}^{(i,t+1)} p_{L,s}^{(i,t)} + p_{U,s}^{(i,t+1)} p_{L,s}^{(i,t+1)}}{4} \quad (4)$$

For the BEC it is possible to compute analytic expressions for the exact (extrinsic) probability of erasure of convolutional encoders, using the method proposed in [12] and [13]. Here, we use this method to derive the exact expressions for the transfer functions of the component decoders. DE is then performed by tracking the evolution of $p_a^{(i,t)}$ with the number of iterations, with the initialization $p_{U,s}^{(0,t)} = p_{U,p}^{(0,t)} = p_{L,s}^{(0,t)} = p_{L,p}^{(0,t)} = 0$ for $t = 0$ and $t > L$, and 1 otherwise. The BP threshold corresponds to the maximum channel parameter ϵ for which successful decoding is achieved, i.e., $p_a^{(i,t)}$ tends to zero for all time instants t as i tends to infinity.

B. Spatially Coupled Serially Concatenated Codes

Similarly to the parallel case, DE equations can be derived for SC-SCCs. Let $p_{O,s}$ and $p_{I,s}$ be the average (extrinsic) erasure probability on the systematic bits at the output of the outer and inner decoder, respectively. Likewise, we define $p_{O,p}$ and $p_{I,p}$ for the parity bits at the output of the outer and inner decoder, respectively.

The erasure probabilities $p_{I,s}$ and $p_{I,p}$ can be written as

$$p_{I,s}^{(i,t)} = f_{I,s}(q_O^{(i-1)}, \epsilon) \quad (5)$$

$$p_{I,p}^{(i,t)} = f_{I,p}(q_O^{(i-1)}, \epsilon), \quad (6)$$

where

$$q_O^{(i-1)} = \epsilon \cdot \frac{p_{O,s}^{(i-1,t)} + p_{O,p}^{(i-1,t)} + p_{O,s}^{(i-1,t-1)} + p_{O,p}^{(i-1,t-1)}}{4}, \quad (7)$$

and $f_{I,s}$ and $f_{I,p}$ denote the inner decoder transfer functions for the systematic and parity bits, respectively.

Likewise, $p_{O,s}$ and $p_{O,p}$ are

$$p_{O,s}^{(i,t)} = f_{O,s}(q_I^{(i-1)}, q_I^{(i-1)}) \quad (8)$$

$$p_{O,p}^{(i,t)} = f_{O,p}(q_I^{(i-1)}, q_I^{(i-1)}), \quad (9)$$

where

$$q_I^{(i-1)} = \epsilon \cdot \frac{p_{I,s}^{(i-1,t)} + p_{I,s}^{(i-1,t+1)}}{2}. \quad (10)$$

The a-posteriori erasure probability on the information bits at time t after i iterations is

$$p_a^{(i,t)} = \epsilon \cdot p_{O,s}^{(i,t)} \cdot \frac{p_{I,s}^{(i,t)} + p_{I,s}^{(i,t+1)}}{2}. \quad (11)$$

DE is then performed by tracking the evolution of $p_a^{(i,t)}$ with the number of iterations, with the initialization $p_{I,s}^{(0,t)} = p_{I,p}^{(0,t)} = p_{O,s}^{(0,t)} = p_{O,p}^{(0,t)} = 0$ for $t = 0$ and $t > L$ and 1 otherwise.

¹We remark that although (2) is not applied within the DE recursion it is required for the computation of the area bound on the MAP threshold.

C. Spatially Coupled Turbo Codes with Random Puncturing

Higher rates can be obtained by applying puncturing. Here, we consider random puncturing. Assume that a code sequence \mathbf{x} is randomly punctured such that a fraction $\rho \in [0, 1]$ of the coded bits survive after puncturing, and then transmitted over a $\text{BEC}(\epsilon)$. ρ will be referred to as the *permeability rate*. For the BEC, puncturing is equivalent to transmitting \mathbf{x} through a $\text{BEC}(\epsilon_\rho)$ resulting from the concatenation of two BECs, $\text{BEC}(\epsilon)$ and $\text{BEC}(1 - \rho)$, where $\epsilon_\rho = 1 - (1 - \epsilon)\rho$. The DE equations derived in the previous subsections can be easily modified to account for puncturing. Consider first the case of SC-PCCs. We consider only puncturing of the parity bits, and that both C_U and C_L are equally punctured with permeability rate ρ . The code rate of the (uncoupled) punctured parallel concatenated code (PCC) is $R = \frac{1}{1+2\rho}$. This results in a slight modification of the DE equations, substituting $\epsilon \leftarrow \epsilon_\rho$ in (1), (2).

For SC-SCCs we consider puncturing as proposed in [14], [15], which results in better SCCs as compared to standard SCCs. Let ρ_0 and ρ_1 be the permeability rate of the systematic and parity bits, respectively, of C_O sent directly to the channel (see [15, Fig. 1]), and ρ_2 the permeability rate of the parity bits of C_I . The code rate of the (uncoupled) punctured² SCC is $R = \frac{1}{\rho_0 + \rho_1 + 2\rho_2}$. The DE for punctured SC-SCCs is obtained by substituting $\epsilon \leftarrow \epsilon_{\rho_2}$ in (5), (6), and modifying (7) to

$$q_O^{(i-1)} = \frac{\epsilon \cdot \left(p_{O,s}^{(i-1,t)} + p_{O,s}^{(i-1,t-1)} \right) + \epsilon_{\rho_1} \cdot \left(p_{O,p}^{(i-1,t)} + p_{O,p}^{(i-1,t-1)} \right)}{4},$$

and (8), (9) to

$$p_{O,s}^{(i,t)} = f_{O,s} \left(q_I^{(i-1)}, \tilde{q}_I^{(i-1)} \right) \quad (12)$$

$$p_{O,p}^{(i,t)} = f_{O,p} \left(q_I^{(i-1)}, \tilde{q}_I^{(i-1)} \right), \quad (13)$$

where $q_I^{(i-1)}$ is given in (10) and

$$\tilde{q}_I^{(i-1)} = \epsilon_{\rho_1} \cdot \frac{p_{I,s}^{(i-1,t)} + p_{I,s}^{(i-1,t+1)}}{2}. \quad (14)$$

IV. EXTENSION TO LARGER COUPLING MEMORIES

The results from the previous sections can easily be generalized to larger coupling memories $m > 1$.

Let us first consider SC-PCCs. In the general case the information sequences $\mathbf{u}_t, \mathbf{u}_{t-1}, \dots, \mathbf{u}_{t-m}$ from $m+1$ different time instances are used by the encoders at time t . This is achieved by dividing the information sequence \mathbf{u}_t into the sequences $\mathbf{u}_{t,j}$, $j = 0, \dots, m$ by a multiplexer, and also dividing a properly reordered copy of the information bits into $\mathbf{u}_{t,j'}$, $j' = 0, \dots, m$, which can be accomplished by permutation Π_t followed by a multiplexer. At the input of the upper encoder C_U at time t the sequences $\mathbf{u}_{t-j,j}$ are multiplexed and reordered by the permutation Π_t^U . The lower encoder C_L receives the information sequences $\mathbf{u}_{t-j',j'}$,

multiplexed and reordered by Π_t^L . The encoder in Fig. 1(a) corresponds to the special case $m = 1$.

In the DE recursion we now have to modify (3) to

$$q_L^{(i-1)} = \epsilon \cdot \frac{\sum_{j=0}^m \sum_{k=0}^m p_{L,s}^{(i,t+j-k)}}{(m+1)^2},$$

and the a-posteriori erasure probability on the information bits at time t and iteration i (4) becomes

$$p_a^{(i,t)} = \epsilon \cdot \frac{\sum_{j=0}^m \sum_{k=0}^m p_{U,s}^{(i,t+j)} p_{L,s}^{(i,t+k)}}{(m+1)^2}.$$

Likewise, for SC-SCCs the code sequence \mathbf{v}_t^O of C_O is divided randomly into the sequences $\tilde{\mathbf{v}}_{t,j}^O$, $j = 0, \dots, m$. C_I receives at time t the sequences $\tilde{\mathbf{v}}_{t-j,j}^O$ after passing a multiplexer and a permutation. The encoder in Fig. 1(b) corresponds to the special case $m = 1$.

Equations (7) and (10) in the DE recursion are modified accordingly to

$$q_O^{(i-1)} = \epsilon \cdot \frac{\sum_{j=0}^m p_{O,s}^{(i-1,t-j)} + p_{O,p}^{(i-1,t-j)}}{2(m+1)}$$

and

$$q_I^{(i-1)} = \epsilon \cdot \frac{\sum_{j=0}^m p_{I,s}^{(i-1,t+j)}}{m+1}.$$

The a-posteriori erasure probability on the information bits at time t after i iterations (11) becomes

$$p_a^{(i,t)} = \epsilon \cdot p_{O,s}^{(i,t)} \cdot \frac{\sum_{j=0}^m p_{I,s}^{(i,t+j)}}{m+1}.$$

V. RESULTS AND DISCUSSION

In this section, we give numerical results for some SC-TCs, using the DE described in Section III and IV. In our examples we consider SC-TCs with identical rate-1/2, 4-states component encoders. In particular, we consider component encoders with generator polynomials (1, 5/7) in octal notation. For notational simplicity, we denote the uncoupled PCC ensemble by \mathcal{C}_{PCC} and the corresponding coupled ensemble by $\mathcal{C}_{\text{SC-PCC}}$. For SC-SCCs, we denote by \mathcal{C}_{SCC} , and $\mathcal{C}_{\text{SC-SCC}}$ the uncoupled and coupled ensembles, respectively. Note that since the two component encoders are identical, $f_{U,s}(x, y) = f_{L,s}(x, y)$ and $f_{U,p}(x, y) = f_{L,p}(x, y)$ for SC-PCCs, and $f_{I,s}(x, y) = f_{O,s}(x, y)$ and $f_{I,p}(x, y) = f_{O,p}(x, y)$ for SC-SCCs. All presented thresholds correspond to the stationary case $L \rightarrow \infty$, which lower bounds the thresholds for finite L . For small L the threshold can be considerably larger but at the expense of a higher rate loss.

In Table I we give the BP threshold for several SC-TCs and coupling memory $m = 1$ and 3, denoted by ϵ_{SC}^1 and ϵ_{SC}^3 . We also report in the table the BP threshold (ϵ_{BP}) and the MAP threshold (ϵ_{MAP}) of the uncoupled ensembles. The MAP threshold was computed applying the area theorem [16]. In all cases we observe an improvement of the BP threshold when coupling is applied. We remark that for $\mathcal{C}_{\text{SC-PCC}}$ the BP threshold of the uncoupled ensemble is already close to

²In this paper we consider $\rho_0 = 1$, i.e., the overall code is systematic.

TABLE I
THRESHOLDS FOR SC-TCs

Ensemble	Rate	ϵ_{BP}	ϵ_{MAP}	ϵ_{SC}^1	ϵ_{SC}^3
C_{PCC}/C_{SC-PCC}	1/3	0.6428	0.6553	0.6553	0.6553
C_{SCC}/C_{SC-SCC}	1/4	0.6896	0.7483	0.7378	0.7482

TABLE II
THRESHOLDS FOR PUNCTURED SC-TCs

Ensemble	Rate	ϵ_{BP}	ϵ_{MAP}	ϵ_{SC}^1	ϵ_{SC}^3
C_{PCC}/C_{SC-PCC}	1/3	0.6428	0.6553	0.6553	0.6553
C_{SCC}/C_{SC-SCC}	1/3	0.6118	0.6615	0.6519	0.6614
C_{PCC}/C_{SC-PCC}	1/2	0.4606	0.4689	0.4689	0.4689
C_{SCC}/C_{SC-SCC}	1/2	0.4010	0.4973	0.4773	0.4969

the MAP threshold, therefore the potential gain with coupling is limited. However, it is interesting to observe that the BP threshold of C_{SC-PCC} with $m = 1$ is very close to ϵ_{MAP} , suggesting threshold saturation. The results for the ensemble C_{SC-SCC} are also given in Table I for coupling memory $m = 1$ and 3. We observe that the ensemble C_{SCC} has a poor BP threshold as compared to the MAP threshold. This is a well-known phenomenon for SCCs, for which the gap between the BP and the MAP threshold is large. A significant improvement is obtained by applying coupling with $m = 1$. However, there is still a gap between ϵ_{BP} and ϵ_{MAP} , meaning that threshold saturation has not occurred. The BP threshold can be further improved by increasing the coupling memory to $m = 3$. In this case the BP threshold is very close to the MAP threshold, suggesting that threshold saturation occurs for large enough coupling memory. This behavior is similar to the threshold saturation phenomenon of SC-LDPC codes, which occurs for smoothing parameter $w \rightarrow \infty$ [2].

In Table II we show the BP thresholds of punctured SC-TCs, in order to compare SC-PCCs and SC-SCCs for a given code rate. We consider $R = 1/3$ and $R = 1/2$, and coupling memory 1.³ For the SC-SCC we used $\rho_1 = 1$ and $\rho_2 = 0.5$ for $R = 1/3$ and $\rho_1 = 0.2$ and $\rho_2 = 0.4$ for $R = 1/2$. Again, in all cases an improvement of the BP threshold is observed when coupling is applied. As expected, for a given rate the PCC ensemble shows a better threshold than the SCC ensemble. However, the improvement in the BP threshold due to coupling for the latter is very significant. For $R = 1/3$ and $m = 1$ the BP threshold of C_{SC-SCC} is very close to that of the (unpunctured) ensemble C_{SC-PCC} , while a large gap is observed for the uncoupled ensembles. For $m = 3$ C_{SC-SCC} achieves a better BP threshold than C_{SC-PCC} . The result is even more remarkable for $R = 1/2$. In this case, while the uncoupled SCC ensemble shows a very poor threshold, C_{SC-SCC} shows a superior threshold than C_{SC-PCC} already for $m = 1$.

³For $R = 1/3$ the SC-PCC is not punctured.

VI. CONCLUSIONS

In this paper we have introduced some block-wise spatially coupled ensembles of parallel and serially concatenated convolutional codes and performed a density evolution analysis on the BEC. In all considered cases spatial coupling results in an improvement of the BP threshold and our numerical results suggest that threshold saturation occurs if the coupling memory is chosen significantly large. The threshold improvement is larger for the serial ensembles, which are known to have poor BP thresholds without coupling but are stronger regarding the distance spectrum. Puncturing the serial and parallel ensembles to equal code rates, we observe that the threshold of the serial ensemble can surpass the one of the parallel ensemble.

REFERENCES

- [1] A. Jiménez Feltström and K.Sh. Zigangirov, "Periodic time-varying convolutional codes with low-density parity-check matrices," *IEEE Trans. Inf. Theory*, vol. 45, no. 5, pp. 2181–2190, Sept. 1999.
- [2] S. Kudekar, T.J. Richardson, and R.L. Urbanke, "Threshold saturation via spatial coupling: Why convolutional LDPC ensembles perform so well over the BEC," *IEEE Trans. Inf. Theory*, vol. 57, no. 2, pp. 803–834, Feb. 2011.
- [3] M. Lentmaier, A. Sridharan, D.J. Costello, Jr., and K.Sh. Zigangirov, "Iterative decoding threshold analysis for LDPC convolutional codes," *IEEE Trans. Inf. Theory*, vol. 56, no. 10, pp. 5274–5289, Oct. 2010.
- [4] M. Lentmaier, D. Truhachev, and K. Sh. Zigangirov, "To the theory of low density convolutional codes II," *Problems of Information Transmission (Problemy Peredachi Informatsii)*, vol. 37, pp. 15–35, Oct.-Dec. 2001.
- [5] E.K. Hall and S.G. Wilson, "Stream-oriented turbo codes," *IEEE Trans. Inf. Theory*, vol. 47, no. 5, pp. 1813–1831, Jul 2001.
- [6] K. Engdahl, M. Lentmaier, and K. Sh. Zigangirov, "On the theory of low-density convolutional codes," *Lecture Notes in Computer Science (AAECC-13)*, vol. 1719, pp. 77–86, Springer-Verlag, New York 1999.
- [7] A. Huebner, K. Sh. Zigangirov, and D. J. Costello, Jr., "Laminated turbo codes: A new class of block-convolutional codes," *IEEE Trans. Inf. Theory*, vol. 54, no. 7, pp. 3024–3034, July 2008.
- [8] W. Zhang, M. Lentmaier, K.Sh. Zigangirov, and D.J. Costello, Jr., "Braided convolutional codes: a new class of turbo-like codes," *IEEE Trans. Inf. Theory*, vol. 56, no. 1, pp. 316–331, Jan. 2010.
- [9] S. Moloudi and M. Lentmaier, "Density evolution analysis of braided convolutional codes on the erasure channel," in *Proc. IEEE International Symposium on Information Theory*, Honolulu, HI, USA, July 2014.
- [10] C. Berrou, A. Glavieux, and P. Thitimajshima, "Near Shannon limit error-correcting coding and decoding: turbo-codes (1)," in *Proc. IEEE International Conference on Communications*, Geneva, Switzerland, May 1993, vol. 2, pp. 1064–1070.
- [11] S. Benedetto, D. Divsalar, G. Montorsi, and F. Pollara, "Serial concatenation of interleaved codes: performance analysis, design, and iterative decoding," *IEEE Trans. Inf. Theory*, vol. 44, no. 3, pp. 909–926, May 1998.
- [12] B.M. Kurkoski, P.H. Siegel, and J.K. Wolf, "Exact probability of erasure and a decoding algorithm for convolutional codes on the binary erasure channel," in *Proc. IEEE Global Telecommunications Conference, 2003. GLOBECOM '03.*, Dec. 2003, vol. 3.
- [13] J. Shi and S. ten Brink, "Exact EXIT functions for convolutional codes over the binary erasure channel," in *Proceedings of the 44th Allerton Conference on Communication, Control, and Computing*, Monticello, IL, USA, 2006.
- [14] A. Graell i Amat, G. Montorsi, and F. Vatta, "Design and performance analysis of a new class of rate compatible serially concatenated convolutional codes," *IEEE Trans. Commun.*, vol. 57, no. 8, pp. 2280–2289, Aug 2009.
- [15] A. Graell i Amat, L.K. Rasmussen, and F. Brännström, "Unifying analysis and design of rate-compatible concatenated codes," *IEEE Trans. Commun.*, vol. 59, no. 2, pp. 343–351, Feb 2011.
- [16] C. Measson, A. Montanari, T.J. Richardson, and R. Urbanke, "The generalized area theorem and some of its consequences," *IEEE Trans. Inf. Theory*, vol. 55, no. 11, pp. 4793–4821, Nov. 2009.